International Journal of Thermal Sciences 48 (2009) 2331–2340

Contents lists available at ScienceDirect

International Journal of Thermal Sciences

journal homepage: www.elsevier.com/locate/ijts

Effects of variable electric conductivity and non-uniform heat source (or sink) on convective micropolar fluid flow along an inclined flat plate with surface heat flux

M.M. Rahman [a,*], M.J. Uddin [b], A. Aziz [c]

[a] Department of Mathematics and Statistics, College of Science, Sultan Qaboos University, P.O. Box 36, Al-Khod 123, Muscat, Sultanate of Oman
[b] Department of Mathematics, Faculty of Science and Information Technology, Daffodil International University, 102, Shukrabad, Mirpur Road, Dhanmondi, Dhaka-1207, Bangladesh
[c] Department of Mechanical Engineering, School of Engineering and Applied Science, Gonzaga University, Spokane, WA 99258, USA

ARTICLE INFO

Article history:
Received 27 February 2009
Received in revised form
6 May 2009
Accepted 9 May 2009
Available online 13 June 2009

PACS:
44.20.+b
44.25.+f
47.15.Cb
47.50.Cd
47.65.-d

Keywords:
Convective flow
Micropolar fluid
Heat transfer
Electric conductivity
Inclined surface
Locally self-similar solution

ABSTRACT

Numerical simulations have been carried out to investigate the effects of the fluid electric conductivity and non-uniform heat source (or sink) on two-dimensional steady hydromagnetic convective flow of a micropolar fluid (in comparison with the Newtonian fluid) flowing along an inclined flat plate with a uniform surface heat flux. The local similarity solutions are presented for the non-dimensional velocity distribution, microrotation, and temperature profiles in the boundary layer. The significance of the physical parameters on the flow field is discussed in detail. The results show that the values of the skin-friction coefficient and the Nusselt number are higher for the case of constant fluid electric conductivity compared with those for the variable fluid electric conductivity. The effect of temperature dependent heat generation is much stronger than the effect of surface dependent heat generation. The results also show that effects of the fluid electric conductivity and non-uniform heat generation in a micropolar fluid are less pronounced than that in a Newtonian fluid.

1. Introduction

Many transport processes that occur both in nature and in industries involve fluid flows with combined heat and mass transfer. Such flows are driven by the buoyancy effects arising from the density variations caused by the variations in temperature and/or species concentrations. A micropolar fluid contains rotating micro-constituents that cause the fluid to exhibit non-Newtonian behavior. Micropolar fluid models have been found useful in the study of flows of exotic lubricants, colloidal suspensions, polymeric fluids, liquid crystals, additive suspensions, body fluids, turbulent shear flows and flows in capillaries and microchannels.

Ariman et al. [1] have given an excellent review of the micropolar fluid model and its applications. Hoyt and Fabula [2] have shown experimentally that the fluids containing minute polymeric additives can reduce skin friction by 25–30%. This reduction was explained with the theory of micropolar fluids. As shown by Power [3], body fluids such as the fluid in the brain can also be adequately modeled as micropolar fluids.

The free convective flow of the fluids with microstructure is of considerable interest in applications such as liquid crystals, dilute solutions of polymer fluids and many types of suspensions. In these and many other situations, the fluid flow is driven by buoyancy effects occurring in an extensive, uniform fluid flow. Convective flow of micropolar fluids over flat, curved and wavy surfaces has attracted much attention from researchers since the formulation of the flow model by Eringen [4,5]. Many investigators have studied and reported results for micropolar fluids. The notable contributions are from Ebert [6], Jena and Mathur [7], Soundalgekar and

* Corresponding author. Tel.: +968 2414 2247; fax: +968 2414 1490.
E-mail address: mansurdu@yahoo.com (M.M. Rahman).

1290-0729/$ – see front matter © 2009 Elsevier Masson SAS. All rights reserved.
doi:10.1016/j.ijthermalsci.2009.05.003

Nomenclature

Roman

B_0	magnetic induction, [Wb m^{-2}]
C_f	local skin-friction coefficient
c_p	specific heat due to constant pressure, [J kg^{-1} K^{-1}]
f	dimensionless stream function
g_0	acceleration due to gravity, [m s^{-2}]
g	dimensionless microrotation
j	micro-inertia per unit mass, [m^2]
M	local magnetic field parameter
M_w	plate couple stress, [Pa m]
M_x	dimensionless plate couple stress
Nu_x	local Nusselt number
n	microrotation parameter
Pr	Prandtl number
Q	temperature dependent heat source (or sink) parameter
Q^*	surface dependent heat source (or sink) parameter
q_w	surface heat flux, [W m^{-2}]
Re_x	local Reynolds number
S	coefficient of vortex viscosity, [Pa s]
T_w	temperature at the surface of the plate, [K]
T	temperature of the fluid within the boundary layer, [K]
T_∞	temperature of the ambient fluid, [K]
U_∞	free stream velocity, [m s^{-1}]
u,v	the x- and y-component of the velocity field, [m s^{-1}]
x,y	axes in direction along and normal to the plate, [m]

Greek

α	angle of inclination [rad]
β^*	volumetric coefficient of thermal expansion, [K^{-1}]
γ	local buoyancy parameter
ρ	fluid density, [kg m^{-3}]
μ	coefficient of dynamic viscosity, [Pa s]
υ	kinematic coefficient of viscosity, [m^2 s^{-1}]
υ_s	spin-gradient viscosity, [m^2 s^{-1}]
σ	microrotation component normal to xy-plane, [s^{-1}]
σ_0'	electrical conductivity of the fluid [S m^{-1}]
σ_0	magnetic permeability [N A^{-2}]
ψ	stream function, [m^2 s^{-1}]
ξ	micro-inertia density parameter
η	similarity variable
τ_w	wall shear stress, [Pa]
Θ	surface temperature parameter
θ	dimensionless temperature
k	thermal conductivity of fluid, [Wm^{-1} K^{-1}]
Δ	vortex viscosity parameter

Subscripts

w	surface conditions
∞	conditions far away from the surface

Takhar [8], Gorla and Takhar [9], Yucel [10], Gorla [11], Khonsari and Brew [12], Khonsari [13], Gorla et al. [14], Gorla and Nakayam [15], Char and Chang [16] and Raptis [17]. Rees and Pop [18] studied free convection boundary layer flow of micropolar fluids from a vertical flat plate whereas Desseaux and Kelson [19] studied the same flow bounded by a stretching sheet. Mitarai et al. [20] studied collisional granular flow with a micropolar fluid model. El-Arabawy [21] studied effect of suction/injection on the flow of a micropolar fluid past a continuously moving plate in the presence of radiation. Rahman and Sattar [22] studied transient convective flow of micropolar fluid past a continuously moving vertical porous plate in the presence of radiation. Recently, Rahman and Sultana [23] studied radiative heat transfer effects in a micropolar fluid flowing past a vertical porous flat plate with variable surface heat flux. Lately, Rahman [24] studied convective flows of micropolar fluids from radiate isothermal porous surfaces with viscous dissipation and Joule heating.

A number of free convective processes are also driven by heat generation or absorption in the fluid. The heat generation or absorption may be due to chemical reaction and/or dissociation effects in the flowing fluid. The presence of heat generation or absorption may alter the temperature distribution in the fluid which in turn affects the particle deposition rate in systems such as nuclear reactors, electronic chips, and semiconductor wafers. The exact modeling of internal heat generation or absorption is difficult but some simple mathematical models may express its average behavior for most physical situations. Heat generation or absorption has been assumed to be constant, space dependent or temperature dependent. Vajravelu and Hadjinicolaou [25] studied the heat transfer characteristics of the laminar boundary layer of a viscous fluid over a stretching sheet with viscous dissipation or frictional heating and temperature dependent internal heat generation included in the analysis. Rahman and Sattar [26] studied magnetohydrodynamic heat and mass transfer processes from a plate with an oscillatory velocity and a constant heat source. Molla et al. [27] studied natural convection flow along a heated wavy surface with a temperature dependence heat source. Mohammadein and Gorla [28] investigated heat transfer in a micropolar fluid over a stretching sheet with viscous dissipation and internal heat generation. Rahman and Sattar [29] studied magnetohydrodynamic convective flow of a micropolar fluid past a continuously moving vertical porous plate in the presence of heat generation or absorption. Aforementioned studies include only the effect of uniform heat generation or absorption i.e. temperature dependent heat generation or absorption on heat transfer. Abo-Eldahab and El-Aziz [30] have included the effect of non-uniform heat source but confined to the case of viscous fluids only.

Jones [31] investigated the free convection problem of a Newtonian fluid over an inclined flat plate with a positive angle of inclination. He developed two series solutions, one valid near the leading edge and the other at large distances from the leading edge. A step-by-step numerical solution was also obtained to cover the intermediate region where neither series solutions applied. Garg and Jayaraj [32] studied the effect of thermophoresis on aerosol particles in laminar flow over an inclined plate. Alam et al. [33–37] published a series of papers on inclined plate investigating the effects of thermophoresis on the viscous flow models under various flow conditions. All of the afore-mentioned works for the inclined plate assumed a constant electric conductivity of the fluid. To the best of our knowledge, the problem of a micropolar fluid of variable electric conductivity flowing over an inclined plate with non-uniform heat source (or sink) in the presence of uniform heat flux boundary condition has remained unexplored.

In the present study we extend the work of Rahman and Sattar [29] and analyze the flow of a variable electric conductivity micropolar fluid with non-uniform heat source (or sink) over an inclined impermeable flat plate subject to a uniform surface heat

flux boundary condition. The resulting governing equations are solved numerically to obtain the local similarity solutions. Graphical results for non-dimensional velocity, microrotation and temperature profiles including local skin-friction coefficient and the local Nusselt number in tabular form are presented for a range of values of the parameters characterizing the flow. The accompanying discussion provides physical interpretations of the results.

2. Flow analysis

Consider a steady two-dimensional hydromagnetic laminar convective flow of a viscous, incompressible, micropolar fluid along a semi-infinite inclined impermeable flat plate with an acute angle α to the vertical. The applied magnetic field is assumed to be in the y-direction and varies in strength as a function of x and is defined as:

$$\vec{B} = (0, B(x)). \tag{1}$$

The flow configurations and the coordinate system are shown in Fig. 1.

The external electric field is assumed to be zero and the magnetic Reynolds number is assumed to be small. Hence, the induced magnetic field is small compared with the externally applied magnetic field. The fluid of density (ρ) is quiescent ($U_\infty = 0$) and the convective motion is induced by the buoyancy forces. The viscosity of the fluid (μ) is assumed to be constant. The pressure gradient, body forces, viscous dissipation and Joule heating effects are neglected compared with the effect of internal heat source (or sink).

Within the framework of the above-noted assumptions, the convective flow of a steady incompressible micropolar fluid subject to the Boussinesq approximation can be described by the following conservation equations (see Rees and Pop [18], Rahman and Sattar [29]):

Continuity Equation:

$$\frac{\partial u}{\partial x} + \frac{\partial v}{\partial y} = 0, \tag{2}$$

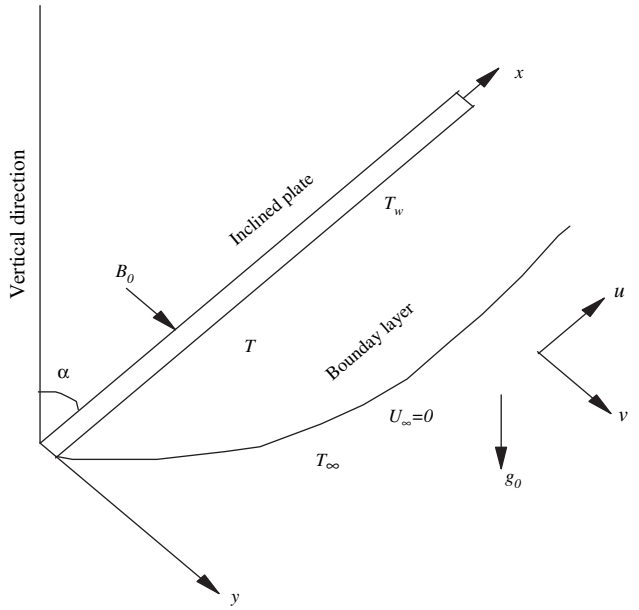

Fig. 1. Flow configurations and the coordinate system.

Momentum Equation:

$$u\frac{\partial u}{\partial x} + v\frac{\partial u}{\partial y} = \left(\upsilon + \frac{S}{\rho}\right)\frac{\partial^2 u}{\partial y^2} + \frac{S}{\rho}\frac{\partial \sigma}{\partial y} + g_0\beta(T - T_\infty)\cos\alpha - \frac{\sigma_0'(B(x))^2 u}{\rho}, \tag{3}$$

Angular Momentum Equation:

$$u\frac{\partial \sigma}{\partial x} + v\frac{\partial \sigma}{\partial y} = \frac{\upsilon_s}{\rho j}\frac{\partial^2 \sigma}{\partial y^2} - \frac{S}{\rho j}\left(2\sigma + \frac{\partial u}{\partial y}\right), \tag{4}$$

Energy Equation:

$$\rho c_p\left(u\frac{\partial T}{\partial x} + v\frac{\partial T}{\partial y}\right) = k\frac{\partial^2 T}{\partial y^2} + q''', \tag{5}$$

where u,v are the velocity components along x,y co-ordinates respectively, $\upsilon = \mu/\rho$ is the kinematic viscosity, ρ is the mass density of the fluid, μ is the dynamic viscosity, $\upsilon_s = (\mu + S/2)j$ (see Ahmadi [38]) is the microrotation viscosity or spin-gradient viscosity, S is the microrotation coupling coefficient (also known as the coefficient of gyro-viscosity or the vortex viscosity), σ is the microrotation component normal to the xy-plane, j is the micro-inertia per unit mass, T is the temperature of the fluid in the boundary layer, c_p is the specific heat of the fluid at constant pressure, k is the fluid thermal conductivity, g_0 is the acceleration due to gravity, β is the volumetric coefficient of thermal expansion. In the present work, we assume that the micro-inertia per unit mass j is a constant. The non-uniform heat source/sink q''' [see [30]) is modeled as

$$q''' = \frac{\kappa U_0}{2\upsilon x}\left[Q(T - T_\infty) + Q^*(T_w - T_\infty)e^{-\eta}\right], \tag{6}$$

where Q and Q^* are the coefficients of space and temperature dependent heat source/sink respectively and T_∞ is the temperature of the fluid outside the boundary layer, η is defined in equation (12). Here we note that the case $Q > 0$, $Q^* > 0$ corresponds to heat source and that $Q < 0$, $Q^* < 0$ corresponds to heat sink.

For the flow under study, we assume that the strength of the applied magnetic field $B(x)$ is variable and has the form (see Helmy [39]):

$$B(x) = \frac{B_0}{\sqrt{x}}, \quad \text{where } B_0 \text{ is a constant.} \tag{7}$$

Moreover, the electrical conductivity σ_0' is assumed to be dependent on the velocity of the fluid and has the form (see Helmy [39]):

$$\sigma_0' = \sigma_0 u, \text{ where } \sigma_0 \text{ is a constant.} \tag{8}$$

The term $\sigma_0'(B(x))^2 u/\rho$ taking into account (7) and (8) can be written as:

$$\frac{\sigma_0'(B(x))^2 u}{\rho} = \frac{\sigma_0 B_0^2 u^2}{\rho x}. \tag{9}$$

Using equation (9), the momentum equation (3) can be written as:

$$u\frac{\partial u}{\partial x} + v\frac{\partial u}{\partial y} = \left(\upsilon + \frac{S}{\rho}\right)\frac{\partial^2 u}{\partial y^2} + \frac{S}{\rho}\frac{\partial \sigma}{\partial y} + g_0\beta(T - T_\infty)\cos\alpha - \frac{\sigma_0 B_0^2 u^2}{\rho x}. \tag{10}$$

2.1. Boundary conditions

The appropriate boundary conditions for our model are

(i) On the plate surface ($y = 0$):

$$u = 0,\ v = 0 (\text{no-slip and impermeable wall conditions}) \tag{11a}$$

$$\sigma = -n\frac{\partial u}{\partial y} (\text{microrotation proportional to vorticity}) \tag{11b}$$

and

$$\frac{\partial T}{\partial y} = -\frac{q_w}{\kappa} (\text{uniform surface heat flux}) \tag{11c}$$

(ii) Matching with the quiescent free stream ($y \to \infty$):

$$u = U_\infty = 0, \quad \sigma = 0, \quad T = T_\infty, \tag{11d}$$

where the subscripts w and ∞ refer to the wall and boundary layer edge, respectively. A linear relationship between the microrotation function σ and the surface shear $\partial u/\partial y$ is chosen for investigating the effect of different surface conditions for microrotation. When microrotation parameter $n = 0$, we obtain $\sigma = 0$ which represents no-spin condition i.e. the microelements in a concentrated particle flow-close to the wall are not able to rotate as stipulated by Jena and Mathur [7]). The case n=0.5 represents vanishing of the anti-symmetric part of the stress tensor and represents weak concentration. For this case Ahmadi [38]) suggested that in a fine particle suspension, the particle spin is equal to the fluid velocity at the wall. The case corresponding of $n = 1$ is representative of the turbulent boundary layer flows (see Peddison and McNitt [40]).

2.2. Dimensionless equations

We introduce the following dimensionless variables:

$$\eta = y\sqrt{\frac{U_0}{2\upsilon x}}, \psi = \sqrt{2\upsilon U_0 x} f(\eta), \sigma = \sqrt{\frac{U_0^3}{2\upsilon x}} g, \theta(\eta) = \frac{T - T_\infty}{T_w - T_\infty} \tag{12}$$

where ψ is the stream function, U_0 is some reference velocity and $T_w - T_\infty = q_w/k\sqrt{2\upsilon x/U_0}$.

Since $u = \partial\psi/\partial y$ and $v = -\partial\psi/\partial x$ we have from equation (12) that,

$$u = U_0 f' \quad \text{and} \quad v = -\sqrt{\frac{\upsilon U_0}{2x}}(f - \eta f'). \tag{13}$$

Here f is non-dimensional stream function and prime denotes differentiation with respect to η.

Now introducing equations (12) and (13) into equations (10) and (4)–(5), we obtain,

$$(1 + \Delta)f''' + ff'' + \Delta g' + \gamma\theta\cos\alpha - Mf'^2 = 0, \tag{14}$$

$$\left(1 + \frac{1}{2}\Delta\right)\xi g'' - 2\Delta(2g + f'') + \xi(f'g + g'f) = 0, \tag{15}$$

$$\theta'' + \Pr(f\theta' - f'\theta) + \left(Q\theta + Q^* e^{-\eta}\right) = 0. \tag{16}$$

where

$\Delta = S/\mu$ is the vortex viscosity parameter, $\xi = jU_0/\upsilon x$ is the micro-inertia density parameter, $\gamma = 2g_0\beta x(T_w - T_\infty)/U_0^2$ is the buoyancy parameter, $M = 2\sigma_0 B_0^2/\rho$ is the magnetic field parameter and $\Pr = \mu c_p/k$ is the Prandtl number.

The corresponding boundary conditions (11) become,

$$\left.\begin{array}{l} f = f' = 0, g = -nf'', \theta' = -1 \text{ at } \eta = 0, \\ f' = 0, g = 0, \theta = 0 \qquad \text{as } \eta \to \infty. \end{array}\right\} \tag{17}$$

Because the parameters ξ and γ depend on the coordinate x, the solutions are *locally similar*. Such local similarity analyses have been performed by many authors (see for example Raptis [17], El-Arabawy [21], Rahman and Sattar [29], Alam et al. [33–37,41], Chamka [42], Cortell [43,44], Hayat et al. [45] and Aziz [46]) and the results found to be accurate. We treat equations (14)–(16) as ordinary differential equations and solve them to derive *locally* similar solutions for a range of values of the physical parameters characterizing the flow.

2.3. Skin-friction coefficient and Nusselt number

The quantities of engineering interest are the skin-friction coefficient and the Nusselt number. The local skin-friction coefficient is defined as

$$C_f = \left(2\mathrm{Re}_x^{-1}\right)^{\frac{1}{2}}[1 + (1 - n)\Delta]f''(0), \tag{18}$$

$$\text{or, } C_f^* = f''(0) \text{ where } C_f^* = \frac{\mathrm{Re}_x^{1/2}}{\sqrt{2}[1 + (1.0 - n)\Delta]}C_f. \tag{19}$$

The Nusselt number is given by

$$Nu_x = \left(2^{-1}\mathrm{Re}_x\right)^{\frac{1}{2}}\frac{1}{\theta(0)}, \tag{20}$$

$$\text{or, } Nu_x^* = \frac{1}{\theta(0)} \text{ where } Nu_x^* = \sqrt{2}\mathrm{Re}^{\frac{-1}{2}}Nu_x. \tag{21}$$

The numerical values of C_f^* and Nu_x^* are calculated from equations (19) and (21), respectively.

3. Numerical solution

The set of equations (14)–(16) is highly nonlinear and coupled and therefore the system cannot be solved analytically. The nonlinear systems (14)–(16) with boundary conditions (17) are solved using the Nachtsheim and Swigert [47] shooting iteration technique. For a brief discussion of the Nachtsheim–Swigert shooting iteration technique, the readers may also consult the work of Rahman [24], Alam et al. [41]. Thus adopting this numerical technique, a computer program was set up for the solutions of the governing non-linear ordinary differential equations of our problem with a sixth order Runge–Kutta method of integration.

3.1. Code verification

For viscous fluid flow ($\Delta = \xi = 0$) and $\gamma = 0$ equation (14) reduces to the equation (6) of Cortell [48] and equation (8) of Hayat et al. [45] if we replace our magnetic field parameter M by $M = 2n/n + 1$ where n is the nonlinear stretching parameter (see Cortell [48]). To assess the accuracy of the present code, we tabulate the values of $-f''(0)$ for a viscous fluid in Table 1 and compare them with the numerical results reported by Cortell [48] and Hayat et al. [45]. Table 1 shows that the values produced by the present code and those by Cortell [48] and Hayat et al. [45] are in good agreement.

It is also worth noting that for $Q = Q^* = 0$, equation (16) reduces to the equation (27) of Cortell [43] if we put $m = 13$, $k = 1.0$, $E_c' = 0$ and $\sigma = 32\Pr$ in his equation (27). For viscous fluid flow we have

Table 1
Comparison of the values of $-f''(0)$ for viscous fluid when $\Delta = \xi = \gamma = 0$ with Cortell [48] and Hayat et al. [45].

n	Cortell [48]	Hayat et al. [45]	Present
0.0	0.627547	0.627555	0.627498
0.2	0.766758	0.766837	0.767066
0.5	0.889477	0.889544	0.892366
0.75	0.953786	0.953975	0.956365
1.0	1.000000	1.000000	1.002125
1.5	1.061587	1.066160	1.063424
3.0	1.148588	1.148593	1.150085
7.0	1.216847	1.216850	1.218111
10.0	1.234875	1.234875	1.236074
20.0	1.257418	1.257424	1.258574
100.0	1.276768	1.276774	1.277862
∞	–	–	1.282887

calculated the value of $\theta(0) = 1.022866$ which is in agreement with $\theta(0) = 1.02151$ of Cortell [43]. This close agreement validates the accuracy of the present code.

In order to verify the effect of the integration step size $\Delta\eta$, we tested the code with three different step sizes namely; $\Delta\eta = 0.001$, $\Delta\eta = 0.002$, and $\Delta\eta = 0.003$. In each case, we found excellent agreement among the results. Fig. 2(a)–(c), respectively, show the velocity, the microrotation, and the temperature profiles for the three step sizes. The results for the three different step sizes are graphically indistinguishable. It was found that $\Delta\eta = 0.001$ provided sufficiently accurate results and further refinement of the grid size was therefore not warranted.

4. Results and discussion

For the purpose of discussing the results, the numerical calculations are presented in the form of non-dimensional velocity, microrotation and temperature profiles. In these calculations, the values of the buoyancy parameter γ, Prandtl number Pr, magnetic field parameter M, angle of inclination α, temperature dependent heat source (or sink) parameter Q, surface dependent heat generation (or sink) parameter Q^*, vortex viscosity parameter Δ, and microrotation parameter n were varied. The choice of the values of the parameters was dictated by the values chosen by the previous investigators. Because of the lack of experimental data for micro-inertia density parameter and vortex viscosity parameter, suitable representative values were chosen in order to determine the polar effects on the flow characteristics. In the simulation the values of the Prandtl number are chosen as 0.73, 2.97, 4.24 and 7 those correspond to air, methyl chloride, sulfur dioxide, and water, respectively. The default values of the other parameters are mentioned in Fig. 2.

Fig. 3(a) shows the velocity profiles for different values of Prandtl number Pr for a cooled plate. As the Prandtl number increases, viscous forces tend to suppress the buoyancy forces and cause the velocity in the hydrodynamic boundary layer to decrease. For small Pr, the boundary layer is thick. For large Pr values the velocity is found to decrease monotonically and the boundary layer thickness is seen to decrease. It is also observed that the maximum values of the velocity are 1.5357, 0.7729, 0.6522 and 0.5143 for $\mathrm{Pr} = 0.73$, 2.97, 4.24 and 7.0, respectively, and occur at $\eta = 0.953$, 0.950, 0.960 and 0.976, respectively. It is seen that the maximum

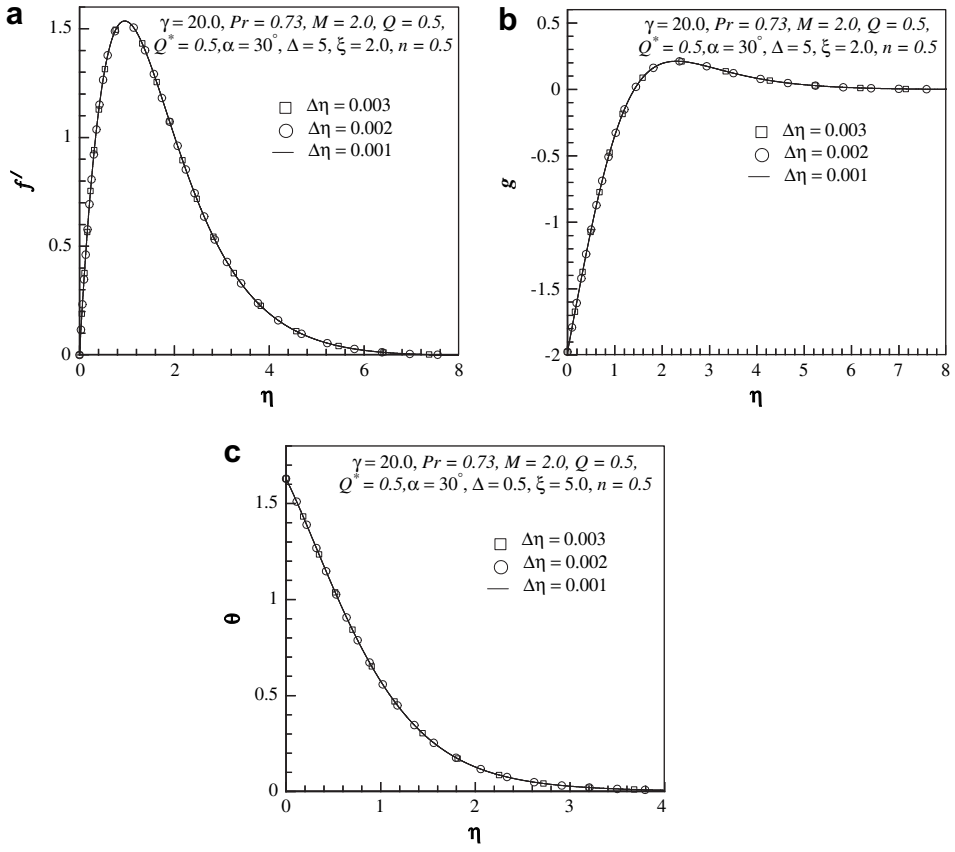

Fig. 2. (a) Velocity, (b) microrotation, and (c) temperature profiles for different values of $\Delta\eta$.

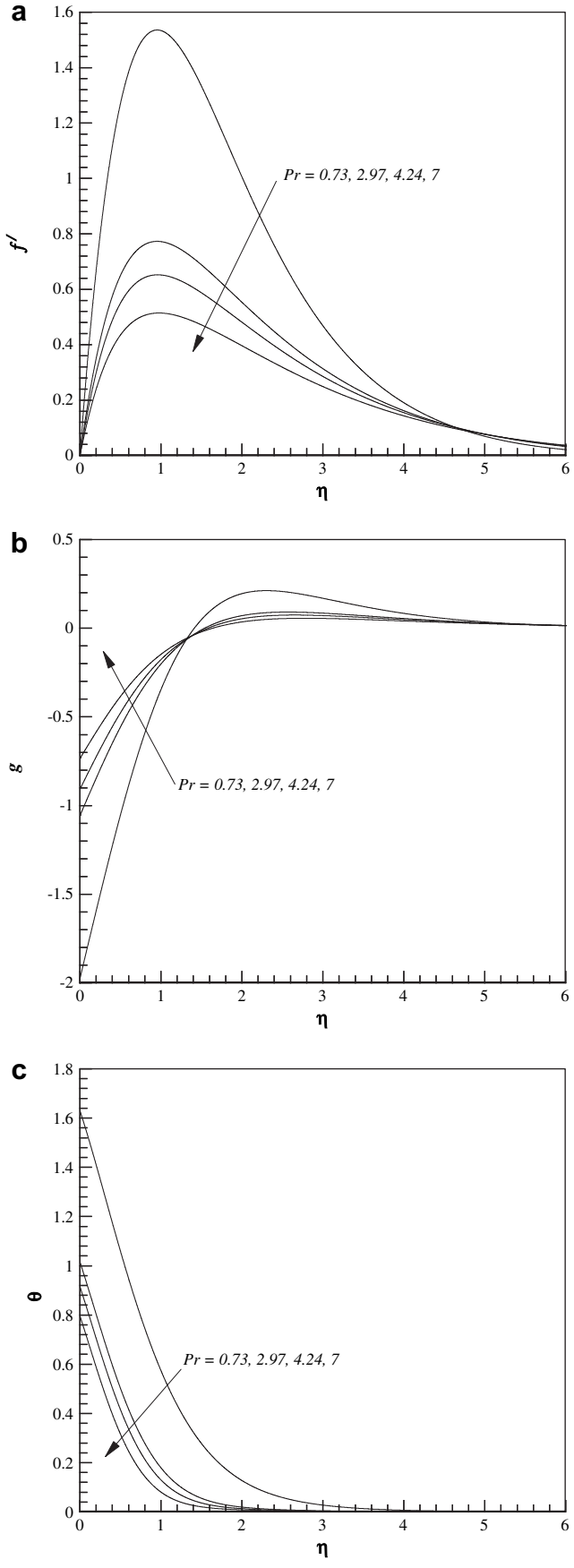

Fig. 3. Variations of non-dimensional (a) velocity (b) microrotation and (c) temperature profiles for different values of Pr.

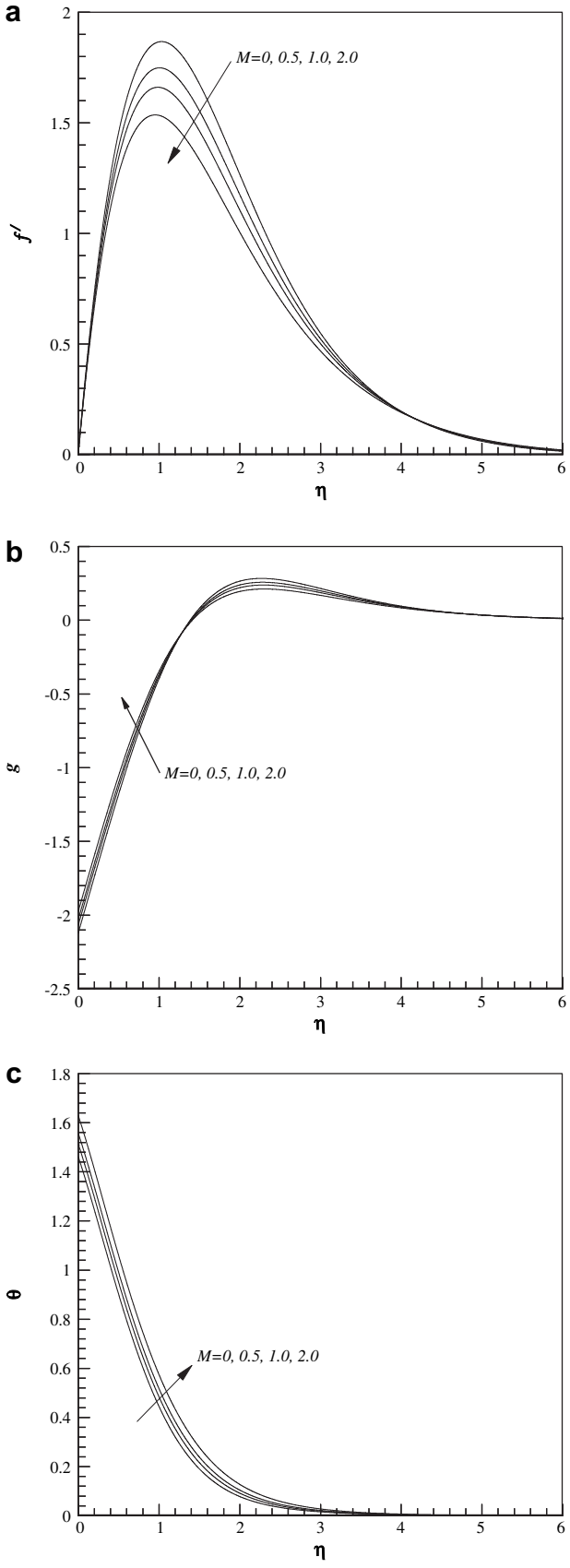

Fig. 4. Variations of non-dimensional (a) velocity (b) microrotation and (c) temperature profiles for different values of *M*.

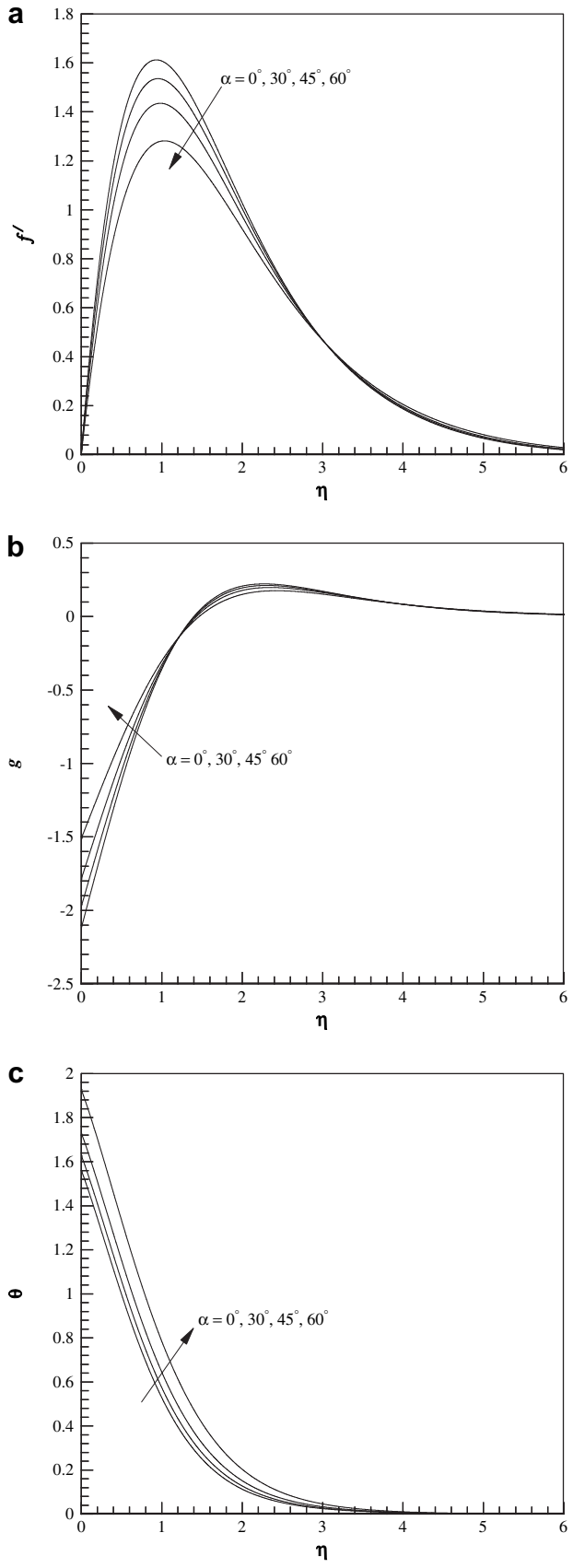

Fig. 5. Variations of non-dimensional (a) velocity (b) microrotation and (c) temperature profiles for different values of α.

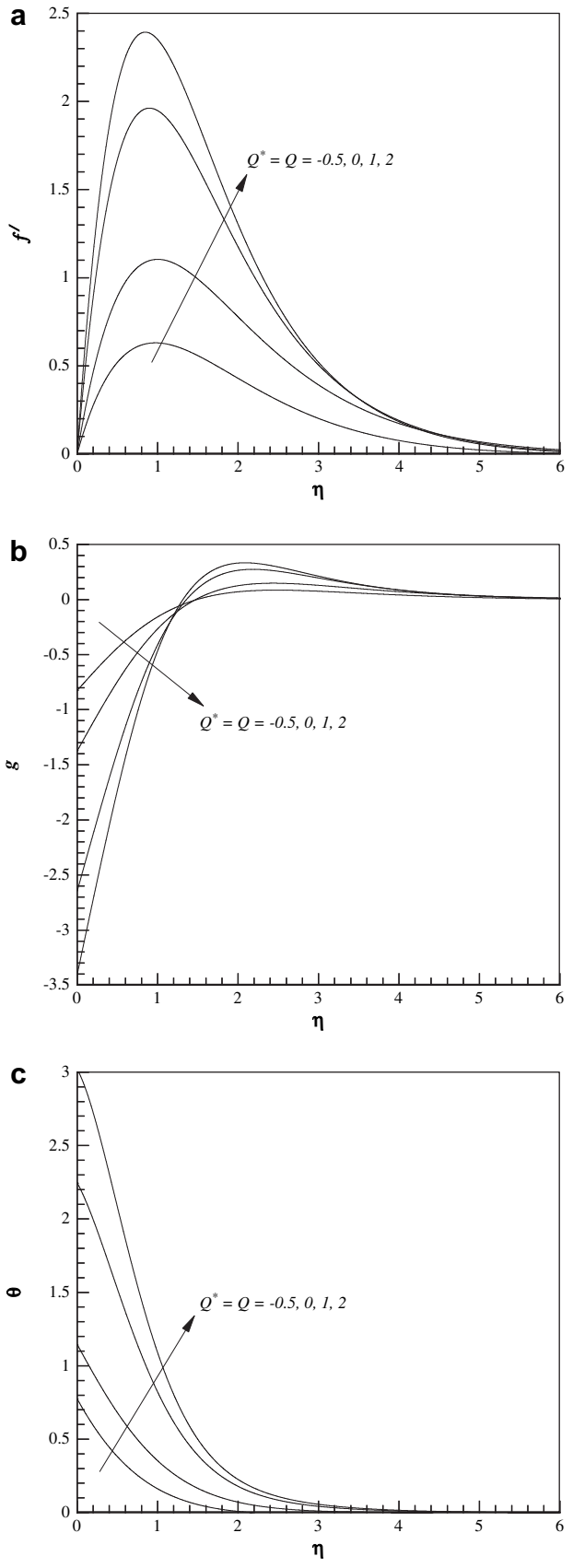

Fig. 6. Variations of non-dimensional (a) velocity (b) microrotation and (c) temperature profiles for different values of Q and Q^*.

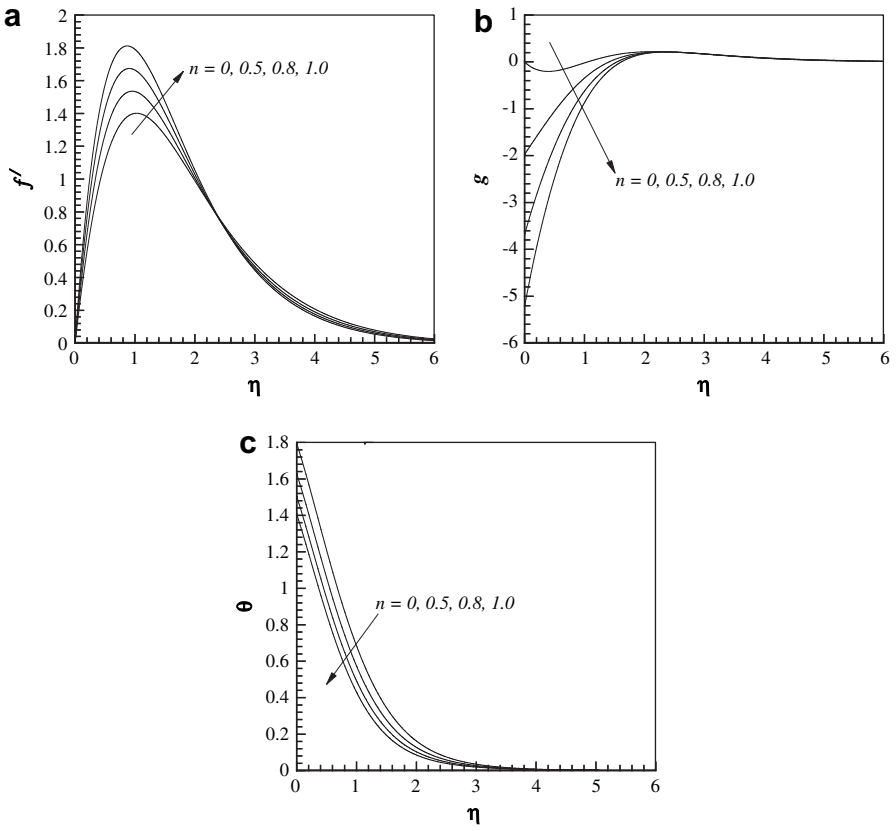

Fig. 7. Variations of non-dimensional (a) velocity, (b) microrotation and (c) temperature profiles for different values of n.

velocity decreases by 66.5% when Pr increases from 0.73 to 7.0. Fig. 3(b) shows the microrotation profiles for the various values of the Prandtl number Pr. From this figure it can be seen that when the plate is cooled, microrotation increases with the increase in Prandtl number. It is also observed that away from the plate ($\eta \geq 1.5$) these profiles overlap. Fig. 3(c) shows the effect of Prandtl number on the temperature profiles. This figure reveals that the effects of the Prandtl number on the thermal boundary layer are similar to those found in the hydrodynamic boundary layer. Furthermore, the maximum values of the temperature are observed to be 1.6289, 1.0145, 0.9143 and 0.7952 for Pr = 0.73, 2.97, 4.24 and 7.0, respectively and they all occur at the surface of the plate. The maximum temperature decreases by 51.18% as Pr increases from 0.733 to 7.0.

Fig. 4(a)–(c), respectively, show the velocity, microrotation and temperature profiles for different values of magnetic field parameter M. From Fig. 4(a) we note that the velocity decreases with the increase of the magnetic field parameter indicating that the magnetic field tends to retard the convective motion of the fluid. This effect is stronger near the surface of the plate. From Fig. 4(b) we see that very close to the plate $\eta \leq 1$, microrotation increases with the increase of the magnetic field parameter. As we move away from the plate, the effect of M becomes less pronounced. Fig. 4(c) reveals that the temperature in the thermal boundary layer increases with the increase of M. This is due to the fact that the magnetic field tends to retard the velocity field, which in turn reduces the heat transfer. This is manifested with higher temperatures in the thermal boundary layer. These results clearly demonstrate that the magnetic field can be used as a means of controlling the flow and heat transfer characteristics.

The effect of the angle of inclination α on the velocity field is shown in Fig. 5(a). From this figure we see that the velocity decreases with the increase of α. As α increases, the effect of the buoyancy force decreases because of the multiplication factor $\cos\alpha$ and the velocities decrease. Fig. 5(b) shows the effect of α in the microrotation profiles. We observe that the angle of inclination α strongly affects the microrotation near the plate surface. Away from the plate, however, the microrotation profiles are minimally affected by the angle of inclination. Fig. 5(c) shows that as the angle of inclination increases, the thermal boundary layer thickens and the temperatures rise.

Fig. 6(a)–(c), respectively, shows the velocity, microrotation and temperature profiles for different values of temperature dependent and surface dependent heat source (or sink) parameters Q and Q^*. Positive values of Q and Q^* represent the heat source i.e. heat generation in the fluid and negative values of Q and Q^* represent the heat sink or heat absorption in the fluid. From Fig. 6(a) it is observed that when the heat is generated ($Q,Q^* > 0$) the buoyancy force increases giving rise to higher velocities in the boundary layer.

Table 2
Values of C_f^* and Nu_x^* for various values of M.

M	Micropolar fluid				Newtonian fluid			
	C_f^*		Nu_x^*		C_f^*		Nu_x^*	
	VEC	CEC	VEC	CEC	VEC	CEC	VEC	CEC
0.0	4.2427	4.2427	0.6841	0.6841	8.9889	8.9889	0.8957	0.8957
0.2	4.1950	4.2079	0.6740	0.6768	8.8172	8.8925	0.8763	0.8847
0.5	4.1352	4.1606	0.6607	0.6665	8.6125	8.7603	0.8511	0.8690
0.8	4.0859	4.1185	0.6493	0.6570	8.4527	8.6410	0.8296	0.8541
1.0	4.0574	4.0927	0.6424	0.6509	8.3641	8.5679	0.8169	0.8446
1.5	3.9973	4.0353	0.6270	0.6371	8.1869	8.4042	0.7892	0.8223
2.0	3.9488	3.9859	0.6139	0.6245	8.0533	8.2640	0.7661	0.8019

However, when heat absorption occurs, the buoyancy force decreases and the flow velocities are reduced. Fig. 6(b) shows that as Q and Q^* increases, the microrotation decreases. When heat generation occurs in the fluid, one would expect the temperature in the thermal boundary layer to increase. This corroborated by Fig. 6(c) where it is seen that the temperatures do indeed increase as Q and Q^* increases.

Fig. 7(a) shows the velocity profiles for different values of microrotation parameter, n. The increase in n results higher flow velocities. Thus the flow is more vigorous in a strongly concentrated micropolar fluid compared with the flow in a weakly concentrated micropolar fluid. Fig. 7(b) shows the microrotation profiles for different values of n. For $n=0$, microrotation remains slightly positive throughout the boundary layer. As n increases, microrotation becomes progressively more negative. The effect is strongest near the plate and diminishes in the far flow field. Fig. 7(c) shows that temperature field is not significantly affected by n.

In Table 2 we present skin-friction coefficient and rate of heat transfer of micropolar fluid and compare them with the results for a Newtonian fluid for various values of the magnetic field parameter for the cases of variable fluid electric conductivity (VEC) as well as of constant fluid electric conductivity (CEC). From this table it is clear that both the skin-friction and heat transfer rate are higher for the case of CEC than for the VEC for the micropolar as well as the Newtonian fluid. It is also worth noting that compared with the Newtonian fluid; the skin friction values as well as heat transfer rate for a micropolar fluid are smaller.

Table 3 shows the skin-friction coefficient and rate of heat transfer of micropolar fluid in comparison with the Newtonian fluid for various values of the angle of inclination α for the cases of variable fluid electric conductivity (VEC) as well as of constant fluid electric conductivity (CEC). This table reveals that skin-friction coefficient as well as rate of heat transfer decreases with the increase of α in both the cases of VEC and CEC. It is also notable that values of these physical parameters are markedly less for a micropolar fluid than the Newtonian fluid.

In Table 4 we present skin-friction coefficient and rate of heat transfer of micropolar fluid in comparison with the Newtonian fluid for various values of the temperature dependent heat source (or sink) parameter (Q) and space dependent heat source (or sink) parameter (Q^*) for the cases of variable fluid electric conductivity (VEC) as well as of constant fluid electric conductivity (CEC). This table shows that skin-friction coefficients corresponding to VEC case are smaller than those of CEC for all increasing values of Q and Q^*. When Q increases from 0 to 1 skin-friction coefficient for micropolar fluid increases by 48% (for the case of VEC) and 49% (for the case of CEC) while for similar increase of Q^* the corresponding change in skin-friction coefficient is 29% (for case of VEC) and 31% (for the case of CEC). For a Newtonian fluid, the values of the skin-friction coefficient are higher than those values of the micropolar fluid. But the rate of increase of skin-friction coefficient for Newtonian fluid is lower compared to the micropolar fluid when Q and Q^* both increases from 0 to 1. Table 4 also depicts that rate of heat transfer from the inclined surface to the micropolar fluid reduces by 34% (for the case of VEC) and 32% (for the case of CEC) when Q increases from 0 to 1 whereas this reduction is 23% (for the case of VEC) and 21% (for the case of CEC) when Q^* increases from 0 to 1. But for a Newtonian fluid the rate of heat transfer decreases by 27% (for the case of VEC) and 23% (for the case of CEC) when Q changes from 0 to 1. Similarly rate of heat transfer decreases by 22% (for the case of VEC) and 17% (for the case of CEC) when Q^* increases from 0 to 1. This table clearly demonstrates that rate of heat transfer strongly depends on the temperature dependent heat source parameter than the space dependent heat source parameter. The opposite effect observed for the case of heat absorption.

Table 3
Values of C_f^* and Nu_x^* for various values of α.

α (in degree)	Micropolar fluid				Newtonian fluid			
	C_f^*		Nu_x^*		C_f^*		Nu_x^*	
	VEC	CEC	VEC	CEC	VEC	CEC	VEC	CEC
0	4.2424	4.2932	0.6403	0.6536	8.6944	8.9544	0.7970	0.8377
30	3.9488	3.9859	0.6139	0.6245	8.0533	8.2640	0.7661	0.8019
45	3.5731	3.5942	0.5777	0.5848	7.2353	7.3869	0.7238	0.7529
60	3.0215	3.0233	0.5188	0.5201	6.0401	6.1152	0.6550	0.6733

Table 4
Values of C_f^* and Nu_x^* for various values of Q and Q^*.

Q^*	Q	Micropolar fluid				Newtonian fluid			
		C_f^*		Nu_x^*		C_f^*		Nu_x^*	
		VEC	CEC	VEC	CEC	VEC	CEC	VEC	CEC
0.5	0.0	3.2631	3.2694	0.7475	0.7495	6.9857	7.1438	0.8892	0.9115
0.5	0.2	3.5160	3.5364	0.6931	0.6983	7.3842	7.5670	0.8395	0.8670
0.5	0.5	3.9488	3.9859	0.6139	0.6245	8.0533	8.2640	0.7661	0.8019
0.5	0.8	4.4529	4.4978	0.5389	0.5552	8.8181	9.0403	0.6945	0.7391
0.5	1.0	4.8320	4.8756	0.4919	0.5119	9.3865	9.6046	0.6484	0.6988
0.0	0.5	3.4170	3.4248	0.7072	0.7109	7.0045	7.1110	0.8818	0.9066
0.2	0.5	3.6409	3.6602	0.6655	0.6725	7.4456	7.5944	0.8301	0.8601
0.5	0.5	3.9488	3.9859	0.6139	0.6245	8.0533	8.2640	0.7661	0.8019
0.8	0.5	4.2313	4.2862	0.5718	0.5851	8.6119	8.8826	0.7138	0.7536
1.0	0.5	4.4083	4.4751	0.5477	0.5623	8.9627	9.2726	0.6839	0.7257
−0.5	0.0	2.1078	2.0475	1.0728	1.0539	4.7629	4.7003	1.2534	1.2427
−0.5	−0.2	1.9066	1.8318	1.1605	1.1404	4.4524	4.3614	1.3279	1.3133
−0.5	−0.5	1.6536	1.5612	1.2893	1.2691	4.0470	3.9172	1.4372	1.4189
−0.5	−0.8	1.4486	1.3453	1.4132	1.3945	3.7023	3.5188	1.5431	1.5132
−0.5	−1.0	1.3336	1.2264	1.4927	1.4754	3.3500	3.3027	1.6116	1.5913
0.0	−0.5	2.5656	2.1890	1.0417	1.0299	5.1898	5.1626	1.1780	1.8717
−0.2	−0.5	2.0355	1.9564	1.1255	1.1101	4.7634	4.6917	1.2679	1.2602
−0.5	−0.5	1.6536	1.5612	1.2893	1.2691	4.0470	3.9172	1.4372	1.4189

5. Conclusions

In this paper numerical simulations have been carried out for the two-dimensional steady boundary layer equations for hydromagnetic convective heat transfer flow of micropolar fluid flowing along a heated inclined flat plate with variable electric conductivity and uniform surface heat flux in the presence of non-uniform heat source (or sink). Using the conventional similarity transformations, the governing partial differential equations have been transformed into non-linear, coupled ordinary differential equations and are solved to obtain locally similar solutions using Nachtsheim–Swigert shooting iteration technique combined with a sixth order Runge–Kutta initial value solver.

We investigated how the flow field, angular velocity (microrotation) of the micro-constituents and temperature field are affected by the variations of the Prandtl number Pr, magnetic field parameter M, heat source (or sink) parameters Q and Q^*, angle of inclination α, and microrotation parameter n and discussed the results. From the present simulations the final remarks can be listed as

1. Skin-friction coefficient (viscous drag) decreases monotonically with the increase of the magnetic field parameter M and the angle of inclination α whereas it increases with the increase of the temperature dependent heat source parameter Q and surface dependent heat source parameter Q^*.

2. The Nusselt number (rate of heat transfer) decreases with the increase of the magnetic field parameter M, temperature dependent heat source parameter Q and surface dependent heat source parameter Q^*, and angle of inclination α.
3. Effect of the temperature dependent heat source parameter Q on the skin-friction coefficient and rate of heat transfer is stronger than the corresponding effect of the surface dependent heat source parameter Q^*.
4. Space and temperature dependent heat absorption are better suited for cooling purposes.
5. Values of the skin-friction coefficient and Nusselt number are higher for the case of constant fluid electric conductivity than the case of variable fluid electric conductivity.
6. The effects of the fluid electric conductivity and non-uniform heat generation on the micropolar fluid are less pronounced compared with the Newtonian fluid.

Acknowledgement

We would like to thank the anonymous referees for their valuable comments which have incorporated to improve the paper.

References

[1] T. Ariman, M.A. Turk, N.D. Sylvester, Microcontinuum fluid mechanics – a review, Int. J. Eng. Sci. 12 (1974) 273.
[2] J.W. Hoyt, A.G. Fabula, The Effect of Additives on Fluid Friction, US Naval Ordnance Test Station Report, 1964.
[3] H. Power, Micropolar fluid model for the brain fluid dynamics, in: Intl. Conf. on bio-fluid mechanics, U.K., 1998.
[4] A.C. Eringen, Theory of micropolar fluids, J. Appl. Math. Mech. 16 (1966) 1–18.
[5] A.C. Eringen, Theory of thermomicrofluids, J. Math. Anal. Appl. 38 (1972) 480–496.
[6] F. Ebert, A similarity solution for the boundary layer flow of a polar fluid, Chem. Eng. J. 5 (1973) 85–92.
[7] S.K. Jena, M.N. Mathur, Similarity solution for laminar free convection flow of thermo-micropolar fluid past a non-isothermal vertical flat plate, Int. J. Eng. Sci. 19 (1981) 1431–1439.
[8] V.M. Soundalgekar, H.S. Takhar, Flow of a micropolar fluid on a continuous moving plat, Int. J. Eng. Sci. 21 (1983) 961–965.
[9] R.S.R. Gorla, H.S. Takhar, Free convection boundary layer flow of a micropolar fluid past slender bodies, Int. J. Eng. Sci. 25 (1987) 949–962.
[10] A. Yucel, Mixed convection micropolar fluid flow over horizontal plate with surface mass transfer, Int. J. Eng. Sci. 27 (1989) 1593–1608.
[11] R.S.R. Gorla, Mixed convection in a micropolar fluid from a vertical surface with uniform heat flux, Int. J. Eng. Sci. 30 (1992) 349–358.
[12] M.M. Khonsari, D. Brew, On the performance of finite journal bearing lubricated with micropolar fluids, ASLE Tribology Trans. 32 (1989) 155–160.
[13] M.M. Khonsari, On the self-excited whirl orbits of a journal in a sleeve bearing lubricated with micropolar fluids, Acta Mech. 81 (1990) 235–244.
[14] R.S.R. Gorla, P.P. Lin, A.J. Yang, Asymptotic boundary layer solutions for mixed convection from a vertical surface in a micropolar fluid, Int. J. Eng. Sci. 28 (1990) 525–533.
[15] R.S.R. Gorla, S. Nakayam, Combined convection from a rotating cone to micropolar fluids, Math. Model. Sci. Comput. 25 (1993) 949–962.
[16] M.I. Char, C.L. Chang, Laminar free convection flow of micropolar fluids from a curved surface, J. Phys. D Appl. Phys. 28 (1995) 1324–1331.
[17] A. Raptis, Flow of a micropolar fluid past a continuously moving plate by the presence of radiation, Int. J. Heat Mass Transf. 41 (1998) 2865–2866.
[18] D.A.S. Rees, I. Pop, Free convection boundary layer flow of micropolar fluid from a vertical flat plat, IMA J. Appl. Math. 61 (1998) 179–197.
[19] A. Desseaux, N.A. Kelson, Flow of a micropolar fluid bounded by a stretching sheet, ANZIAM J. 42 (E) (2000) C536–C560.
[20] N. Mitarai, H. Hayakawa, H. Nakanishi, Collisional granular flow as a micropolar fluid, Phys. Rev. Lett. 88 (2002) 174301–174304.
[21] H.A.M. El-Arabawy, Effect of suction/injection on the flow of a micropolar fluid past a continuously moving plate in the presence of radiation, Int. J. Heat Mass Transf. 46 (2003) 1471–1477.
[22] M.M. Rahman, M.A. Sattar, Transient convective flow of micropolar fluid past a continuously moving vertical porous plate in the presence of radiation, Int. J. App. Math. Egng. 12 (2007) 497–513.
[23] M.M. Rahman, T. Sultana, Radiative heat transfer flow of micropolar fluid with variable heat flux in a porous medium, Nonlinear Anal. Model. Control 13 (2008) 71–87.
[24] M. Rahman, Convective flows of micropolar fluids from radiate isothermal porous surfaces with viscous dissipation and Joule heating, Comm. Nonlinear Sci. Numer. Simulat. 14 (2009) 3018–3030.
[25] K. Vajravelu, A. Hadjinicolaou, Heat transfer in viscous fluid over a stretching sheet with viscous dissipation and internal heat generation, Int. Comm. Heat Mass Tran. 20 (1993) 417–430.
[26] M.M. Rahman, M.A. Sattar, MHD free convection and mass transfer flow with oscillatory plate velocity and constant heat source in a rotating frame of reference, Dhaka Univ. J. Sci. 47 (1999) 63–73.
[27] M.M. Molla, M.A. Hossain, L.S. Yao, Natural convection flow along a vertical wavy surface with uniform surface temperature in presence of heat generation/absorption, Int. J. Therm. Sci. 43 (2004) 157–163.
[28] A.A. Mohammadein, R.S.R. Gorla, Heat transfer in a micropolar fluid over a stretching sheet with viscous dissipation and internal heat generation, Int. J. Num. Meth. Heat Fluid Flow 11 (2001) 50–58.
[29] M.M. Rahman, M.A. Sattar, Magnetohydrodynamic convective flow of a micropolar fluid past a continuously moving vertical porous plate in the presence of heat generation/absorption, ASME J. Heat Transf. 128 (2006) 142–152.
[30] E.M. Abo-Eldahab, M.A. El-Aziz, Blowing/suction on hydromagnetic heat transfer by mixed convection from an inclined continuously stretching surface with internal heat generation/absorption, Int. J. Therm. Sci. 43 (2004) 709–719.
[31] D.R. Jones, Free convection from a semi-infinite flat plate inclined at a small angle to the horizontal, Quart. J. Mech. Appl. Math. 128 (1973) 77–98.
[32] V.K. Garg, S. Jayaraj, Thermophoresis of aerosol particles in laminar flow over inclined plates, Int. J. Heat Mass Transf. 31 (1988) 875–890.
[33] M.S. Alam, M.M. Rahman, M.A. Sattar, MHD free convective heat and mass transfer flow past an inclined surface with heat generation, Thammasat Int. J. Sci. Technol. 11 (2006) 1–8.
[34] M.S. Alam, M.M. Rahman, M.A. Sattar, Effects of thermophoresis and chemical reaction on unsteady hydro magnetic free convection and mass transfer flow past an impulsively started infinite inclined porous plate in the presence of heat generation/absorption, Thammasat Int. J. Sci. Technol. 12 (2007) 44–52.
[35] M.S. Alam, M.M. Rahman, M.A. Sattar, Effects of variable suction and thermophoresis on steady MHD combined free-forced convective heat and mass transfer flow a semi-infinite permeable inclined plat in the presence of thermal radiation, Int. J. Therm. Sci. 47 (2008) 758–765.
[36] M.S. Alam, M.M. Rahman, M.A. Sattar, On the effectiveness of viscous dissipation and Joule heating on steady magnetohydrodynamic heat and mass transfer flow over an inclined radiate isothermal permeable surface in the presence of thermophoresis, Comm. Nonlinear Sci. Numer. Simulat. 14 (2009) 2132–2143.
[37] M.S. Alam, M.M. Rahman, M.A. Sattar, Effects of chemical reaction and thermophoresis on magneto-hydrodynamic mixed convective heat and mass transfer flow along an inclined plate in the presence of heat generation and (or) absorption with viscous dissipation and Joule heating, Can. J. Phys. 86 (2008) 1057–1066.
[38] G. Ahmadi, Self-similar solution of incompressible micropolar boundary layer flow over a semi- infinite plate, Int. J. Eng. Sci. 14 (1976) 639–646.
[39] K.A. Helmy, MHD boundary layer equations for power law fluids with variable electric conductivity, Meccanica 30 (1995) 187–200.
[40] J. Peddison, R.P. McNitt, Boundary layer theory for micropolar fluid, Recent Adv. Eng. Sci. 5 (1970) 405–426.
[41] M.S. Alam, M.M. Rahman, M.A. Samad, Numerical study of the combined free-forced convection and mass transfer flow past a vertical porous plate in a porous medium with heat generation and thermal diffusion, Nonlinear Anal. Model. Control 11 (2006) 331–343.
[42] A.J. Chamka, Thermal radiation and buoyancy effects on hydrodynamic flow over an accelerating permeable surface with heat source or sink, Int. J. Eng. Sci. 38 (2000) 1699–1712.
[43] R. Cortell, Effects of viscous dissipation and radiation on the thermal boundary layer over a nonlinearly stretching sheet, Phys. Lett. A 372 (2008) 631–636.
[44] R. Cortell, Similarity solutions for flow and heat transfer of a quiescent fluid over a nonlinearly stretching surface, J. Mater. Process. Technol. 203 (2008) 176–183.
[45] T. Hayat, Z. Abbas, T. Javed, Mixed convection flow of micropolar fluid over a nonlinearly stretching sheet, Phys. Lett. A 372 (2008) 637–647.
[46] A. Aziz, A similarity solution for laminar thermal boundary layer over a flat plate with a convective surface boundary condition (short communication), Comm. Nonlinear Sci. Numer. Simulat. 14 (2009) 1064–1068.
[47] P.R. Nachtsheim, P. Swigert, Satisfaction of the Asymptotic Boundary Conditions in Numerical Solution of the System of Non-linear Equations of Boundary Layer Type, NASA TND-3004, 1965.
[48] R. Cortell, Viscous flow and heat transfer over a nonlinearly stretching sheet, Appl. Math. Comput. 184 (2007) 864–873.